THE JOURNAL OF PHYSICAL CHEMISTRY LETTERS
A JOURNAL OF THE AMERICAN CHEMICAL SOCIETY

pubs.acs.org/JPCL

Letter

Multi-Particle Three-Dimensional Covariance Imaging: "Coincidence" Insights into the Many-Body Fragmentation of Strong-Field Ionized D_2O

Felix Allum, Chuan Cheng, Andrew J. Howard, Philip H. Bucksbaum, Mark Brouard, Thomas Weinacht, and Ruaridh Forbes*

Cite This: *J. Phys. Chem. Lett.* 2021, 12, 8302−8308

Read Online

ACCESS | Metrics & More | Article Recommendations | Supporting Information

ABSTRACT: We demonstrate the applicability of covariance analysis to three-dimensional velocity-map imaging experiments using a fast time stamping detector. Studying the photofragmentation of strong-field doubly ionized D_2O molecules, we show that combining high count rate measurements with covariance analysis yields the same level of information typically limited to the "gold standard" of true, low count rate coincidence experiments, when averaging over a large ensemble of photofragmentation events. This increases the effective data acquisition rate by approximately 2 orders of magnitude, enabling a new class of experimental studies. This is illustrated through an investigation into the dependence of three-body D_2O^{2+} dissociation on the intensity of the ionizing laser, revealing mechanistic insights into the nuclear dynamics driven during the laser pulse. The experimental methodology laid out, with its drastic reduction in acquisition time, is expected to be of great benefit to future photofragment imaging studies.

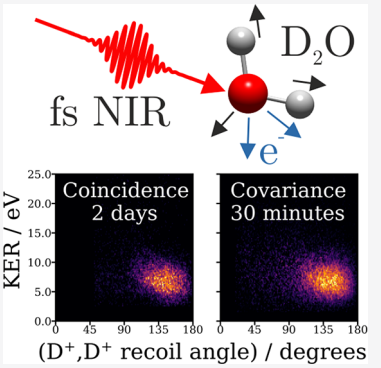

A comprehensive understanding of the interaction between molecules and high intensity laser fields presents a key challenge for the modern chemical physics community.[1,2] A number of ground breaking experimental methods capable of probing molecular photodynamics on the smallest length scales and shortest time scales rely on the interaction between molecules and intense laser fields. Such techniques include high-harmonic spectroscopy,[3−5] laser-induced electron diffraction,[6−8] and Coulomb explosion imaging.[9−13] The latter of these aims to determine nuclear structure on ultrafast time scales through measurement of relative fragment velocities following rapid multiple ionization and subsequent many-body fragmentation. The development of suitable techniques to measure the correlated velocities of charged fragments is crucial for time-resolved Coulomb explosion imaging experiments, as well as experiments probing the fundamental relationship between molecular structure and fragmentation dynamics. Unravelling this relationship can be a difficult task, particularly when ionization is driven by a strong laser field, which initiates a whole host of exotic phenomena that can influence the ultimate photofragmentation dynamics. These include field-induced distortions of molecular energy levels and nuclear dynamics, geometric and dynamic alignment, multielectron ionization dynamics and electron rescattering.[14−17]

To probe the dynamics underlying many-body dissociation of ionized polyatomic molecules and extract nuclear geometric information following fragmentation, it is desirable to not only record the (three-dimensional) velocity vectors of fragments, but the *relative*, *correlated* velocities of two or more fragments.[13,18,19] Typically, this can be achieved by conducting experiments under "coincidence" conditions. By ensuring a very low count rate (<1 parent molecule probed per laser shot), the detection of multiple particles in a given laser shot can be confidently assigned to true coincidences arising from a single molecule.[20,21] As the count rate is increased, signal from "false" coincidences dominates, as multiple molecules are ionized and fragments detected in a single laser shot cannot be assigned to a single molecule. However, as first demonstrated in charged particle experiments by Frasinski and co-workers,[22,23] correlated information can still be extracted by calculating the covariance, a statistical measure of linear correlation, between parameters of interest for two (or three[24−26]) particles across a data set of many laser shots. Covariance between two variables A and B (in our case, three-dimensional ion velocity distributions) is defined as

$$\mathrm{Cov}(A, B) = \langle AB \rangle - \langle A \rangle \langle B \rangle \quad (1)$$

where angled brackets refer to the mean over a series of N observations (in the current work, laser shots). Although performing experiments under high count rate conditions

Received: July 29, 2021
Accepted: August 16, 2021

https://doi.org/10.1021/acs.jpclett.1c02481
J. Phys. Chem. Lett. 2021, 12, 8302−8308

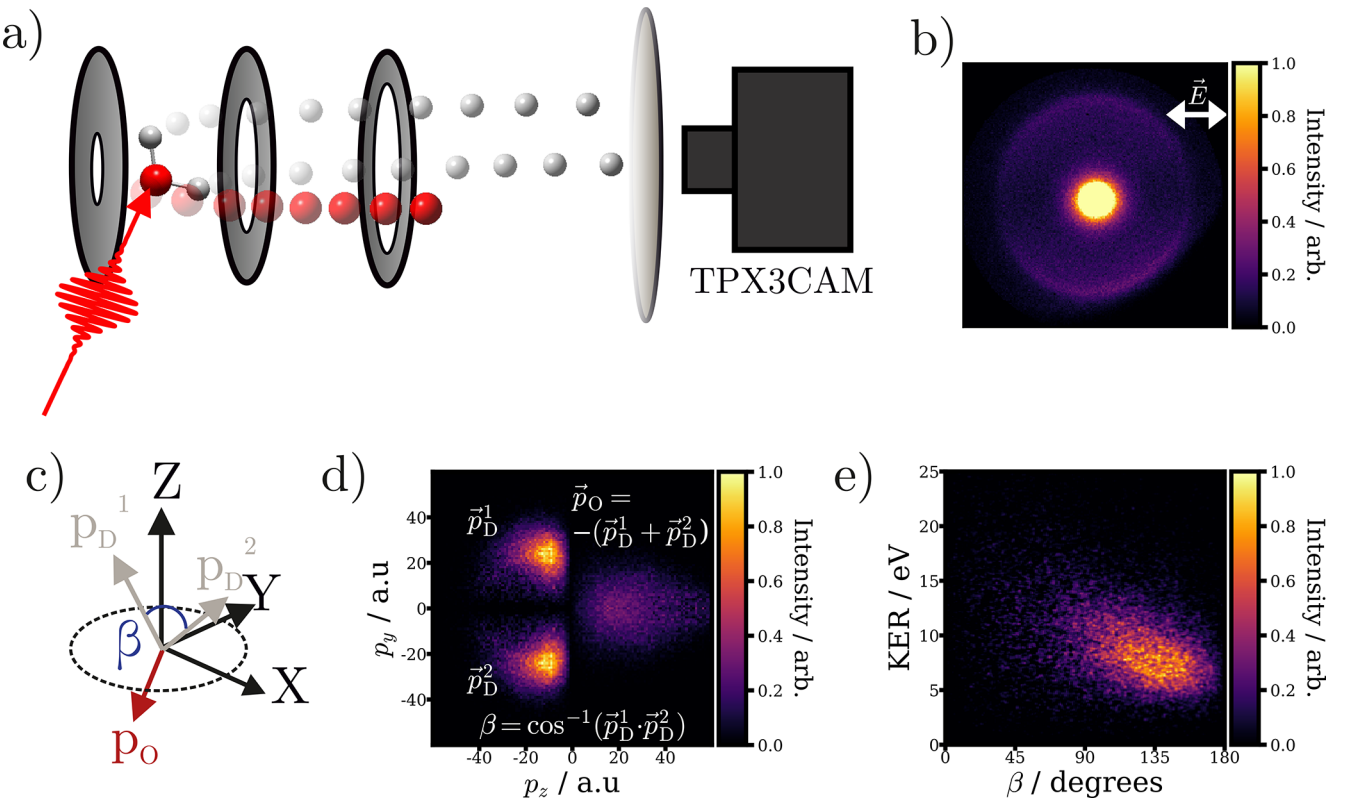

Figure 1. (a) Schematic of the experiment. Ions produced by strong-field ionization of D_2O are accelerated toward a position sensitive detector under velocity-mapping conditions.[43] Panel b displays an example D^+ VMI image, representing a two-dimensional projected velocity distribution. From the recorded momentum distributions in the laboratory (*X*,*Y*,*Z*) frame (illustrated in panel c), correlated information in the molecular/recoil frame can be determined through covariance analysis. (d) Newton plot representation of the correlated momenta of D^+ fragments. (e) (D^+,D^+) covariance intensity plotted as a function of the total kinetic energy release (KER) and the recoil angle between the two D^+ ions, β.

necessarily forfeits event-by-event correlated information afforded by coincidence analysis, the covariance methodology can extract the same correlations when averaging over a large ensemble of observations, as is the case in a typical experiment.[27−30] Following its initial application to time-of-flight mass spectrometry experiments, covariance mapping has been applied to a range of two-dimensional VMI experiments[31−35] and recently a three-dimensional VMI study of the two-body dissociations of CF_3I^{2+}.[36] Recent work by Suits and co-workers combined covariance analysis with a three-dimensional imaging technique to study the Coulomb explosion dynamics of chlorocarbonylsulfenyl chloride molecules.[37] Various applications of covariance analysis have been reviewed recently.[38,39]

Here, we extend the three-dimensional covariance imaging technique to three-body dissociations, using both 2-fold and 3-fold covariance analysis to gain a kinematically complete view of strong-field doubly ionized D_2O. Crucially, these results are compared quantitatively to low count rate experiments performed under otherwise identical experimental conditions.[14−16] In this case, covariance imaging yields the same ensemble-averaged results as those performed under coincidence conditions—with a substantial decrease in experimental acquisition time of approximately 2 orders of magnitude. This facilitates studies that would otherwise be extremely impractical using traditional techniques—as demonstrated through a survey of the effects of peak laser intensity on the many-body breakup of ionized D_2O.[14,15,17,18,40,41] These results elucidate nuclear dynamics driven during the intense laser pulse, and we expect they will stimulate future theoretical work to unravel the complex coupled nuclear and electron dynamics in the strong laser field.[14,42]

The combination of an ion velocity map imaging (VMI) spectrometer equipped with a TPX3CAM camera[44,45] and few-cycle femtosecond laser pulses are exploited to investigate the multiple ionization dynamics of target D_2O molecules, shown schematically in Figure 1a). From the recorded detector positions and arrival times, the three-dimensional laboratory-frame momentum vectors of each ion can be determined (Figure 1c). By correlating this information between two (or three) fragments using covariance analysis, details about fragmentation in the recoil-frame can be determined, shown for the (D^+,D^+) ion pair in panels d and e. In Figure 1d, correlated momentum distributions for the three-body breakup are presented in the form of a Newton plot. Here, the vector bisecting the two D^+ ion momenta is horizontal, and the fragmentation of the three particles is in the plane of the page (i.e., such that p_x = 0). The momentum of the O atom/ion, deduced through momentum conservation, is also plotted. Figure 1e) displays the covariance in a different representation - as a function of the total kinetic energy release (KER), and β, defined as the angle between the two D^+ ions.

Figure 2 compares the correlated momentum distributions of two D^+ ions from D_2O ionized by 10 fs pulses, determined using coincidence and covariance analysis. Once more, both are plotted as a function of β and total KER. Here, data was acquired under two very different conditions: (i) a low count rate regime (~0.007 D^+ ions per laser shot) recorded for

https://doi.org/10.1021/acs.jpclett.1c02481
J. Phys. Chem. Lett. 2021, 12, 8302−8308

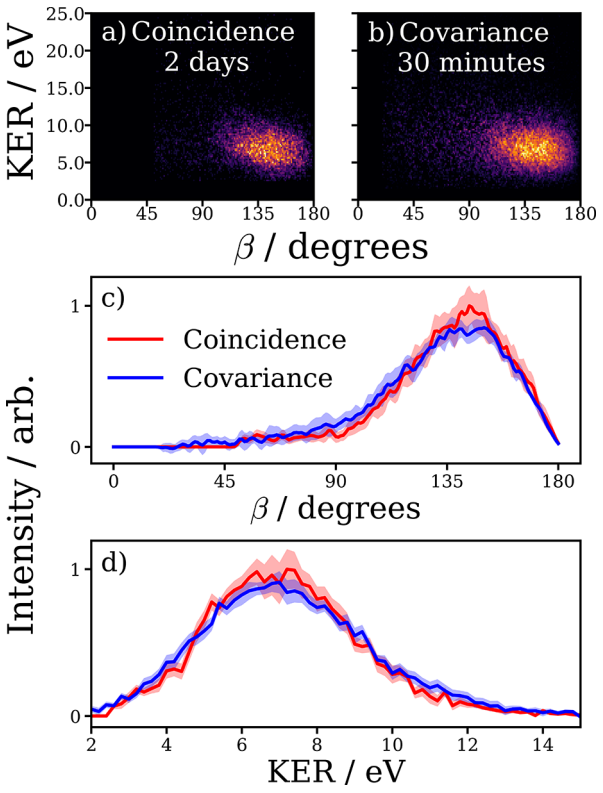

Figure 2. Intensity of the (D^+,D^+) ion pair as a function of total kinetic energy release (KER), and relative angle, β. In panel a, this is determined through coincidence analysis of the low count rate data set, while panel b shows the equivalent covariance analysis of the high count rate data set. The same color scale is used as in Figure 1. Panels c and d further compare the extracted β and KER distributions (normalized by their total area) obtained by summing the two-dimensional arrays in panels a and b over a single axis. Estimated statistical errors (at the 1σ level) of the coincidence and covariance data are represented by the shaded regions.

approximately 2 days and (ii) a high count rate regime (~0.38 D^+ ions per laser shot), recorded for approximately 30 min. Panel a displays the correlation from a coincidence analysis of the low count rate data, while panel b shows the analogous results of calculating the covariance for the high count rate data set. It should be noted that these measurements were not carried out at the maximum count rates for coincidence or covariance. For coincidence measurements, the maximum rate is restricted by the tolerable false coincidence rate. For maximum false coincidence rate of 1%, coincidence measurements can be performed with a count rate about 7 times higher than used here. However, if one were to look at electron−ion coincidences[15] or electron−electron coincidences arising from double ionization, then count rates of these measurements would need to be 10 and 30 times lower, respectively. For covariance, the maximum count rate is determined by the maximum distinguishable number of events of the hit-finding algorithm. If one is limited by 15 hits per shot (a rather conservative estimate, given the higher count rates of previous covariance imaging work[31,32,35]), then the ion−ion covariance measurements could be performed with count rates about 90 times higher. Electron−ion covariance measurements would require count rates about half the value. Thus, in all cases, covariance measurements result in a dramatic decrease in acquisition time, but the exact factor depends on the correlations of interest, and the maximum signal rate that can be tolerated by the detection system.

The results shown in Figure 2a and b are strikingly similar, both in terms of the shape of the correlation island, and the signal-to-noise ratio achieved. This can be seen quantitatively in panels c and d, which compare the extracted KER and β distributions obtained from the coincidence and covariance analysis. Shaded regions correspond to estimated statistical errors in both measurements at a 1σ level (the error estimation method is described in detail in the Supporting Information). A high degree of agreement is achieved, despite the fact that the acquisition time of the low count rate data is roughly one hundred times that of the high count rate data, and that slightly

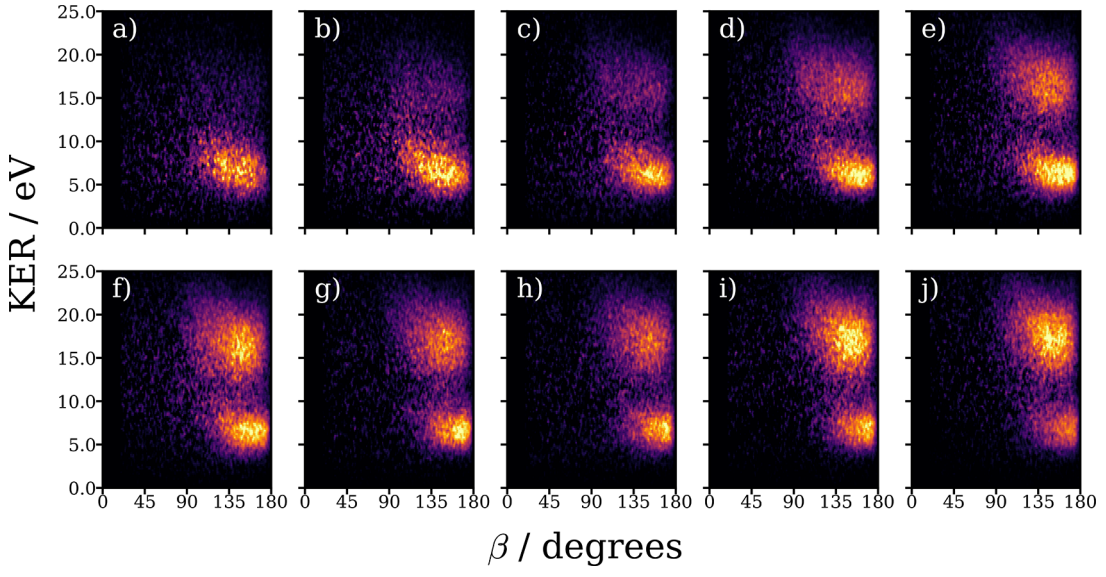

Figure 3. Evolution of the (D^+,D^+) covariance with increasing laser intensity for 30 fs NIR pulses. Each data set was acquired for 20 min under high count rates. The same colors cale is used as in Figure 1. Panels a−j correspond to estimated peak intensities of 120−480 TW cm^{-2}, in intervals of 40 TW cm^{-2}. Systematic changes in these covariance maps can be seen as laser intensity is increased, which are discussed in detail in the main text.

https://doi.org/10.1021/acs.jpclett.1c02481
J. Phys. Chem. Lett. 2021, 12, 8302−8308

fewer total D^+ ions are recorded in the high count rate data set. In the context of experimentally probing photofragmentation dynamics, this has far-reaching consequences. For instance, it enables systematic studies of the effects of laser parameters (e.g., pulse intensity, pulse duration, wavelength) on correlated velocity distributions in a practically achievable time scale.

To demonstrate this, we measured the (D^+,D^+) covariance for 30 fs pulses with different intensities. Recent work has compared the observed three-body dissociation dynamics in D_2O following strong-field ionization by intense 10 and 40 fs pulses.[14,16,41] In these studies, D_2O molecules were found to undergo significant unbending motion during the ionization/fragmentation process for longer laser pulses, characterized by a narrow β distribution in the $D^+/D^+/O$ channel. One possible contribution to this unbending motion is dynamics in states of the monocation. This contribution can be understood in terms of the laser field coupling the (bent) D_0 and (linear) D_1 potentials, inducing bond-softening distortions in the D_0 state.[40,46,47] Additionally, when ionizing with longer pulses (40 fs), the two D^+ were preferentially ejected along the polarization axis of the laser, indicative of dynamic alignment, which was absent for the shorter (10 fs) pulses.[14]

For each intensity, 20 min of data was acquired, enough to determine statistically significant (D^+,D^+) covariances, allowing the entirety of the data to be recorded in a single day. Results are presented in Figure 3, with pulse intensity increasing from panel a to j. Alternative representations of these covariance images are shown in the Supporting Information (Figures S5 and S6). We note two different intensity dependent features in the data. First, a peak at high KER (~13−23 eV), with a fairly broad β distribution, grows in intensity as the pulse intensity is raised. This is due to fragmentation of triply ionized D_2O^{3+} to form $D^+/D^+/O^+$, an assignment which can be unambiguously made using 3-fold covariance analysis, as discussed shortly. The form of the lower KER peak also varies considerably. As the intensity is increased, the β distribution becomes more focused toward 180 deg, indicative of the molecule undergoing greater unbending motion in the laser field.

The results shown in Figure 3 provide a detailed view of the unbending dynamics in strong-field ionized D_2O—highlighting the important role of peak laser intensity, complementing previous studies in this area.[14,16,41] Even with the longer pulses, for which significant nuclear motion during the pulse is possible, very little evidence of this unbending motion is seen in the low intensity regime, which strongly resembles measurements with much shorter pulses (as can be seen in comparing Figure 3a to Figure 2a and b). Likely, this dependence of the fragmentation dynamics on pulse intensity is because for higher intensity pulses, molecules are likely to be ionized earlier in the pulse, and there is a stronger field dressing of states.[18] It is probable that dynamics on both monocation and dication potentials are of importance. As suggested by recent calculations by Yamanouchi and co-workers,[42] if D_2O^{2+} is formed earlier within the pulse envelope (as is likely for higher peak intensities), significantly more unbending occurs prior to dissociation, consistent with the narrowing β distributions seen in Figure 3. Additionally, for all the intensities shown in Figure 3, the high KER feature arising from trication dissociation exhibits a significantly broader β distribution than the lower KER feature, and the β distribution of this feature does not significantly vary with intensity. As noted previously,[14] this is consistent with ionization to the trication while unbending dynamics are occurring in the dication. The β distribution of the trication feature likely reflects the range of geometries at the time of the third and final ionization, shortly after which the molecule fragments rapidly. Dications which are not further ionized continue to unbend prior to three-body dissociation, leading to the observed narrow β distribution centered at 180 deg.

The discussion thus far has concentrated on using covariance imaging to yield correlated velocity information for two ions. In general, however, studying the correlations among three (or more) particles is desirable, particularly for larger molecules, which may break up into many fragments. Three-fold covariance mapping procedures to extract such information are known.[24,26] While observing higher-order correlations is necessarily more challenging than the 2-fold case due to limited detection efficiencies, such analysis is practical and insightful in the current work, even for the 20 min data sets presented in Figure 3. Figure 4 compares results from

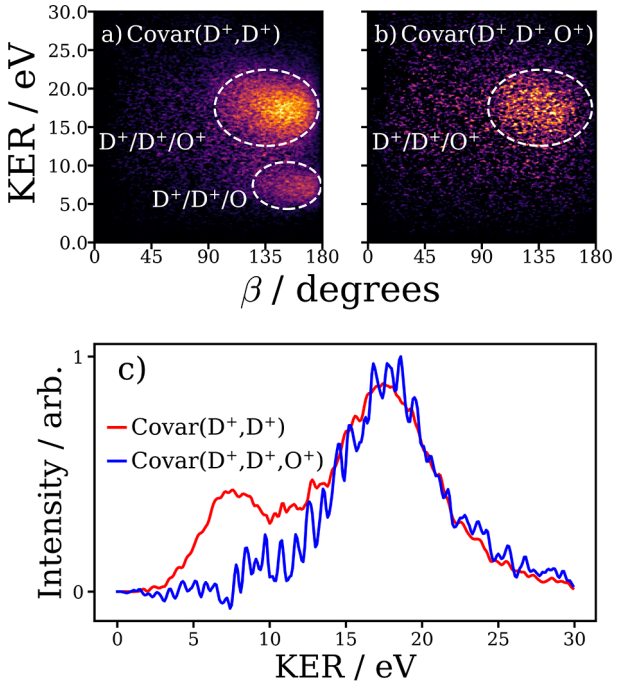

Figure 4. Comparison between (a) the (D^+,D^+) 2-fold covariance and (b) the (D^+,D^+,O^+) 3-fold covariance, for the highest laser intensity 30 fs pulse duration data set. The same color scale is used as in Figure 1. Panel c shows the KER distributions extracted from the 2-fold and 3-fold covariances. Here, the intensity of the 3-fold covariance signal has been divided by 0.26, the estimated detection efficiency of the O^+ ion.

the highest intensity data set using 2-fold (D^+,D^+) covariance analysis and 3-fold (D^+,D^+,O^+) covariance analysis. This can be interpreted as isolating fragmentation channels which produce both two D^+ ions and an O^+ ion. Comparing the two panels definitively confirms the previous assignment of the two distinct features seen. The high KER channel arises from three-body breakup of D_2O^{3+}, and so is visible in both the 2-fold and 3-fold covariances. In contrast, the lower KER feature is absent the 3-fold covariance, as it does not involve production of O^+. This can be clearly seen in the KER distributions shown in Figure 4c). The ratio of intensity of the higher KER feature between 3-fold and 2-fold covariance analysis is 0.26, which is the theoretical detection efficiency of the oxygen ion. A similar

https://doi.org/10.1021/acs.jpclett.1c02481
J. Phys. Chem. Lett. 2021, 12, 8302−8308

number of 0.3 has been obtained through independent analysis of the coincidence data set. The good agreement in the detection efficiency calculation again confirms the convergence of the two methods.

In summary, we have demonstrated a general methodology for high count rate, three-dimensional covariance imaging, applied to many-body photofragmentation dynamics. By benchmarking the technique against experiments performed under coincidence conditions, we establish that equivalent physical insights can be gained from covariance analysis of data acquired at much higher count rates. This greatly enhances the scope of experiments that measure the correlated velocities of two or three fragment ions. In the future, extending the techniques developed here to experiments involving simultaneous detection of electrons and ions[15,48] may be used for (time-resolved) studies utilizing channel- and momentum-resolved above threshold ionization spectroscopy[15,27,49] Finally, we note that while the current work was performed using a MCP/phosphor screen detector coupled to a time stamping TPX3CAM camera, the methodology laid out in this work is universal and can be applied to the hexanode delay line detectors commonly used in coincidence experiments (with the provision that the ultimate upper count rate limit of such detectors is lower than that used in the current work).

METHODS

The experimental apparatus has been described in detail in recent publications,[15,48] and is shown schematically in Figure 1. Briefly, D_2O is introduced into a velocity-map imaging (VMI)[43] spectrometer as a skimmed, effusive molecular beam. Here it is crossed by an intense, femtosecond near-infrared (NIR) laser pulse, focused in the chamber by a curved mirror with a 5 cm focal length. The total count rate was adjusted by altering the number of molecules in the molecular beam, leading to an increased pressure in the interaction region. In the experiments presented in this work, the pulses used were either the 30 fs output of a commercial 1 kHz Ti:sapphire amplifier (centered at 780 nm), or 10 fs pulses produced by compression of pulses using a acousto-optic based pulse shaper[50,51] after spectral broadening in an argon gas filament (centered at 750 nm). The peak intensity in the interaction region is estimated to be 400 TW cm^{-2} for the 10 fs pulses, while for the 30 fs pulses the intensity was varied from 120 to 480 TW cm^{-2}. Ions produced following fragmentation of strong-field ionized D_2O molecules were velocity-mapped to a microchannel plate (MCP)/phosphor screen detector. For experiments carried out at high count rates, the MCP detector was gated in time to prevent detection of D_2O^+ ions. Flashes of light at the detector were imaged by a TPX3CAM camera, capable of recording the arrival time of ion events with ~1 ns resolution,[44,45] enabling full three-dimensional velocity imaging of all ionic fragments.[48] As the impact of a single ion at the detector illuminates multiple pixels of the TPX3CAM over a range of times, hit finding was performed on the data to significantly increase the spatiotemporal resolution.[48]

ASSOCIATED CONTENT

Supporting Information

The Supporting Information is available free of charge at https://pubs.acs.org/doi/10.1021/acs.jpclett.1c02481.

Details of the covariance calculations, example time-of-flight mass spectra, alternative data visualizations, and estimation of covariance errors (PDF)

AUTHOR INFORMATION

Corresponding Author

Ruaridh Forbes − *Stanford PULSE Institute, SLAC National Accelerator Laboratory, Menlo Park, California 94025, United States; Linac Coherent Light Source, SLAC National Accelerator Laboratory, Menlo Park, California 94025, United States;* orcid.org/0000-0003-2097-5991; Email: ruforbes@stanford.edu

Authors

Felix Allum − *Chemistry Research Laboratory, Department of Chemistry, University of Oxford, Oxford OX1 3TA, United Kingdom*

Chuan Cheng − *Department of Physics, Stony Brook University, Stony Brook, New York 11794, United States*

Andrew J. Howard − *Stanford PULSE Institute, SLAC National Accelerator Laboratory, Menlo Park, California 94025, United States*

Philip H. Bucksbaum − *Stanford PULSE Institute, SLAC National Accelerator Laboratory, Menlo Park, California 94025, United States*

Mark Brouard − *Chemistry Research Laboratory, Department of Chemistry, University of Oxford, Oxford OX1 3TA, United Kingdom;* orcid.org/0000-0003-3421-0850

Thomas Weinacht − *Department of Physics, Stony Brook University, Stony Brook, New York 11794, United States*

Complete contact information is available at: https://pubs.acs.org/10.1021/acs.jpclett.1c02481

Notes

The authors declare no competing financial interest.

ACKNOWLEDGMENTS

F.A. thanks the EPSRC for their support. The authors thank Cong Liu for assistance in optimizing the performance of the three-dimensional covariance codes. M.B. gratefully acknowledges support of the EPSRC (Programme Grant No. EP/L005913/1 and EP/V026690/1). A.J.H., R.F., and P.H.B. were supported by the National Science Foundation. A.J.H. was additionally supported under a Stanford Graduate Fellowship as the 2019 Albion Walter Hewlett Fellow. R.F. gratefully ackowledges support from the Linac Coherent Light Source, SLAC National Accelerator Laboratory, which is supported by the US Department of Energy, Office of Science, Office of Basic Energy Sciences, under contract no. DE-AC02-76SF00515. C.C. and T.W. gratefully acknowledge support from the US Department of Energy under Award No. DE-FG02-08ER15984.

REFERENCES

(1) Posthumus, J. H. The dynamics of small molecules in intense laser fields. *Rep. Prog. Phys.* **2004**, *67*, 623−665.

(2) Grossmann, F. *Theoretical Femtosecond Physics: Atoms and Molecules in Strong Laser Fields*, Graduate Texts in Physics; Springer International Publishing, 2018.

(3) Itatani, J.; Levesque, J.; Zeidler, D.; Niikura, H.; Pépin, H.; Kieffer, J. C.; Corkum, P. B.; Villeneuve, D. M. Tomographic imaging of molecular orbitals. *Nature* **2004**, *432*, 867−871.

(4) Haessler, S.; Caillat, J.; Boutu, W.; Giovanetti-Teixeira, C.; Ruchon, T.; Auguste, T.; Diveki, Z.; Breger, P.; Maquet, A.; Carré, B.; et al. Attosecond imaging of molecular electronic wavepackets. *Nat. Phys.* **2010**, *6*, 200−206.
(5) Wörner, H. J.; Bertrand, J. B.; Corkum, P. B.; Villeneuve, D. M. High-harmonic homodyne detection of the ultrafast dissociation of Br_2 molecules. *Phys. Rev. Lett.* **2010**, *105*, 103002.
(6) Meckel, M.; Comtois, D.; Zeidler, D.; Staudte, A.; Pavičić, D.; Bandulet, H. C.; Pépin, H.; Kieffer, J. C.; Dörner, R.; Villeneuve, D. M.; et al. Laser-induced electron tunneling and diffraction. *Science* **2008**, *320*, 1478−1482.
(7) Blaga, C. I.; Xu, J.; Dichiara, A. D.; Sistrunk, E.; Zhang, K.; Agostini, P.; Miller, T. A.; Dimauro, L. F.; Lin, C. D. Imaging ultrafast molecular dynamics with laser-induced electron diffraction. *Nature* **2012**, *483*, 194−197.
(8) Wolter, B.; Pullen, M. G.; Le, A. T.; Baudisch, M.; Doblhoff-Dier, K.; Senftleben, A.; Hemmer, M.; Schröter, C. D.; Ullrich, J.; Pfeifer, T.; et al. Ultrafast electron diffraction imaging of bond breaking in di-ionized acetylene. *Science* **2016**, *354*, 308−312.
(9) Stapelfeldt, H.; Constant, E.; Corkum, P. B. Wave Packet Structure and Dynamics Measured by Coulomb Explosion. *Phys. Rev. Lett.* **1995**, *74*, 3780−3783.
(10) Corrales, M. E.; González-Vázquez, J.; De Nalda, R.; Banares, L. Coulomb Explosion Imaging for the Visualization of a Conical Intersection. *J. Phys. Chem. Lett.* **2019**, *10*, 138−143.
(11) Luzon, I.; Livshits, E.; Gope, K.; Baer, R.; Strasser, D. Making Sense of Coulomb Explosion Imaging. *J. Phys. Chem. Lett.* **2019**, *10*, 1361−1367.
(12) Ding, X.; Forbes, R.; Kübel, M.; Lee, K. F.; Spanner, M.; Naumov, A. Y.; Villeneuve, D. M.; Stolow, A.; Corkum, P. B.; Staudte, A. Threshold photodissociation dynamics of NO_2 studied by time-resolved cold target recoil ion momentum spectroscopy. *J. Chem. Phys.* **2019**, *151*, 174301.
(13) Endo, T.; Neville, S. P.; Wanie, V.; Beaulieu, S.; Qu, C.; Deschamps, J.; Lassonde, P.; Schmidt, B. E.; Fujise, H.; Fushitani, M.; et al. Capturing roaming molecular fragments in real time. *Science* **2020**, *370*, 1072−1077.
(14) Howard, A. J.; Cheng, C.; Forbes, R.; McCracken, G. A.; Mills, W. H.; Makhija, V.; Spanner, M.; Weinacht, T.; Bucksbaum, P. H. Strong-field ionization of water: Nuclear dynamics revealed by varying the pulse duration. *Phys. Rev. A: At., Mol., Opt. Phys.* **2021**, *103*, 043120.
(15) Cheng, C.; Forbes, R.; Howard, A. J.; Spanner, M.; Bucksbaum, P. H.; Weinacht, T. Momentum-resolved above-threshold ionization of deuterated water. *Phys. Rev. A: At., Mol., Opt. Phys.* **2020**, *102*, 052813.
(16) Cheng, C.; Streeter, Z. L.; Howard, A. J.; Spanner, M.; Lucchese, R. R.; Mccurdy, C. W.; Weinacht, T.; Bucksbaum, P. H.; Forbes, R. Strong Field Ionization of Water II: Electronic and Nuclear Dynamics En Route to Double Ionization. *Phys. Rev. A* **2021**, DOI: 10.1021/acs.jpclett.1c02481.
(17) McCracken, G. A.; Bucksbaum, P. H. Ionization induced dynamic alignment of water. *J. Chem. Phys.* **2020**, *152*, 134308.
(18) Légaré, F.; Lee, K. F.; Litvinyuk, I. V.; Dooley, P. W.; Wesolowski, S. S.; Bunker, P. R.; Dombi, P.; Krausz, F.; Bandrauk, A. D.; Villeneuve, D. M.; et al. Laser Coulomb-explosion imaging of small molecules. *Phys. Rev. A: At., Mol., Opt. Phys.* **2005**, *71*, 013415.
(19) Pitzer, M.; Kunitski, M.; Johnson, A. S.; Jahnke, T.; Sann, H.; Sturm, F.; Schmidt, L. P. H.; Schmidt-Böcking, H.; Dörner, R.; Stohner, J.; et al. Direct Determination of Absolute Molecular Stereochemistry in Gas Phase by Coulomb Explosion Imaging. *Science* **2013**, *341*, 1096−1100.
(20) Eland, J. H. Photoelectron-photoion coincidence spectroscopy. I. Basic principles and theory. *Int. J. Mass Spectrom. Ion Phys.* **1972**, *8*, 143−151.
(21) Dörner, R.; Mergel, V.; Jagutzki, O.; Spielberger, L.; Ullrich, J.; Moshammer, R.; Schmidt-Böcking, H. Cold Target Recoil Ion Momentum Spectroscopy: a 'momentum microscope' to view atomic collision dynamics. *Phys. Rep.* **2000**, *330*, 95−192.
(22) Frasinski, L. J.; Codling, K.; Hatherly, P. A. Covariance Mapping: A Correlation Method Applied to Multiphoton Multiple Ionization. *Science* **1989**, *246*, 1029−1031.
(23) Frasinski, L. J.; Stankiewicz, M.; Hatherly, P. A.; Cross, G. M.; Codling, K.; Langley, A. J.; Shaikh, W. Molecular H_2 in intense laser fields probed by electron-electron, electron-ion, and ion-ion covariance techniques. *Phys. Rev. A: At., Mol., Opt. Phys.* **1992**, *46*, R6789−R6792.
(24) Codling, K.; Frasinski, L. J.; Hatherly, P. A.; Stankiewicz, M. New triple coincidence techniques applied to multiple ionisation of molecules. *Phys. Scr.* **1990**, *41*, 433−439.
(25) Frasinski, L. J.; Hatherly, P. A.; Codling, K. Multiphoton multiple ionisation of N_2O probed by three-dimensional covariance mapping. *Phys. Lett. A* **1991**, *156*, 227−232.
(26) Pickering, J. D.; Amini, K.; Brouard, M.; Burt, M.; Bush, I. J.; Christensen, L.; Lauer, A.; Nielsen, J. H.; Slater, C. S.; Stapelfeldt, H. Communication: Three-fold covariance imaging of laser-induced Coulomb explosions. *J. Chem. Phys.* **2016**, *144*, 161105−161105.
(27) Boguslavskiy, A. E.; Mikosch, J.; Gijsbertsen, A.; Spanner, M.; Patchkovskii, S.; Gador, N.; Vrakking, M. J. J.; Stolow, A. The multielectron ionization dynamics underlying attosecond strong-field spectroscopies. *Science* **2012**, *335*, 1336−40.
(28) Mikosch, J.; Patchkovskii, S. Coincidence and covariance data acquisition in photoelectron and -ion spectroscopy. I. Formal theory. *J. Mod. Opt.* **2013**, *60*, 1426−1438.
(29) Mikosch, J.; Patchkovskii, S. Coincidence and covariance data acquisition in photoelectron and -ion spectroscopy. II. Analysis and applications. *J. Mod. Opt.* **2013**, *60*, 1439−1451.
(30) Zhaunerchyk, V.; Frasinski, L. J.; Eland, J. H.; Feifel, R. Theory and simulations of covariance mapping in multiple dimensions for data analysis in high-event-rate experiments. *Phys. Rev. A: At., Mol., Opt. Phys.* **2014**, *89*, 053418.
(31) Slater, C. S.; Blake, S.; Brouard, M.; Lauer, A.; Vallance, C.; John, J. J.; Turchetta, R.; Nomerotski, A.; Christensen, L.; Nielsen, J. H.; et al. Covariance imaging experiments using a pixel-imaging mass-spectrometry camera. *Phys. Rev. A: At., Mol., Opt. Phys.* **2014**, *89*, 011401.
(32) Slater, C. S.; Blake, S.; Brouard, M.; Lauer, A.; Vallance, C.; Bohun, C. S.; Christensen, L.; Nielsen, J. H.; Johansson, M. P.; Stapelfeldt, H. Coulomb-explosion imaging using a pixel-imaging mass-spectrometry camera. *Phys. Rev. A: At., Mol., Opt. Phys.* **2015**, *91*, 053424.
(33) Burt, M.; Amini, K.; Lee, J. W.; Christiansen, L.; Johansen, R. R.; Kobayashi, Y.; Pickering, J. D.; Vallance, C.; Brouard, M.; Stapelfeldt, H. Communication: Gas-phase structural isomer identification by Coulomb explosion of aligned molecules. *J. Chem. Phys.* **2018**, *148*, 091102.
(34) Allum, F.; Burt, M.; Amini, K.; Boll, R.; Köckert, H.; Olshin, P. K.; Bari, S.; Bomme, C.; Brauße, F.; Cunha de Miranda, B.; et al. Coulomb explosion imaging of CH_3I and CH_2ClI photodissociation dynamics. *J. Chem. Phys.* **2018**, *149*, 204313.
(35) Allum, F.; Anders, N.; Brouard, M.; Bucksbaum, P. H.; Burt, M.; Downes-ward, B.; Grundmann, S.; Harries, J.; Ishimura, Y.; Iwayama, H.; et al. Multi-channel photodissociation and XUV-induced charge transfer dynamics in strong-field-ionized methyl iodide studied with time-resolved recoil-frame covariance imaging. *Faraday Discuss.* **2021**, *228*, 571−596.
(36) Lee, J. W. L.; Köckert, H.; Heathcote, D.; Popat, D.; Chapman, R. T.; Karras, G.; Majchrzak, P.; Springate, E.; Vallance, C. Three-dimensional covariance-map imaging of molecular structure and dynamics on the ultrafast timescale. *Commun. Chem.* **2020**, *3*, 72.
(37) Cooper, G. A.; Alavi, S. T.; Li, W.; Lee, S. K.; Suits, A. G. Coulomb Explosion Dynamics of Chlorocarbonylsulfenyl Chloride. *J. Phys. Chem. A* **2021**, *125*, 5481−5489.
(38) Frasinski, L. J. Covariance mapping techniques. *J. Phys. B: At., Mol. Opt. Phys.* **2016**, *49*, 152004.
(39) Vallance, C.; Heathcote, D.; Lee, J. W. L. Covariance-Map Imaging: A Powerful Tool for Chemical Dynamics Studies. *J. Phys. Chem. A* **2021**, *125*, 1117−1133.

(40) Sanderson, J. H.; El-Zein, A.; Bryan, W. A.; Newell, W. R.; Langley, A. J.; Taday, P. F. Geometry modifications and alignment of H_2O in an intense femtosecond laser pulse. *Phys. Rev. A: At., Mol., Opt. Phys.* **1999**, *59*, R2567−R2570.
(41) McCracken, G. A.; Kaldun, A.; Liekhus-Schmaltz, C.; Bucksbaum, P. H. Geometric dependence of strong field enhanced ionization in D_2O. *J. Chem. Phys.* **2017**, *147*, 124308.
(42) Koh, S.; Yamazaki, K.; Kanno, M.; Kono, H.; Yamanouchi, K. Ionization and dissociation dynamics of H_2O in ultrashort intense near-IR laser fields by the time-dependent adiabatic state method and the time-dependent configuration interaction method. *Chem. Phys. Lett.* **2020**, *742*, 137165.
(43) Eppink, A. T. J. B.; Parker, D. H. Velocity map imaging of ions and electrons using electrostatic lenses: Application in photoelectron and photofragment ion imaging of molecular oxygen. *Rev. Sci. Instrum.* **1997**, *68*, 3477−3484.
(44) Fisher-Levine, M.; Nomerotski, A. TimepixCam: A fast optical imager with time-stamping. *J. Instrum.* **2016**, *11*, C03016−C03016.
(45) Nomerotski, A.; Chakaberia, I.; Fisher-Levine, M.; Janoska, Z.; Takacs, P.; Tsang, T. Characterization of TimepixCam, a fast imager for the time-stamping of optical photons. *J. Instrum.* **2017**, *12*, C01017−C01017.
(46) Bucksbaum, P. H.; Zavriyev, A.; Muller, H. G.; Schumacher, D. W. Softening of the H_2^+ molecular bond in intense laser fields. *Phys. Rev. Lett.* **1990**, *64*, 1883−1886.
(47) Rottke, H.; Trump, C.; Sandner, W. Multiphoton ionization and dissociation of H_2O. *J. Phys. B: At., Mol. Opt. Phys.* **1998**, *31*, 1083−1096.
(48) Zhao, A.; Sándor, P.; Weinacht, T. Coincidence velocity map imaging using a single detector. *J. Chem. Phys.* **2017**, *147*, 013922.
(49) Forbes, R.; Boguslavskiy, A. E.; Wilkinson, I.; Underwood, J. G.; Stolow, A. Excited state wavepacket dynamics in NO_2 probed by strong-field ionization. *J. Chem. Phys.* **2017**, *147*, 054305.
(50) Dugan, M. A.; Tull, J. X.; Warren, W. S. High-resolution acousto-optic shaping of unamplified and amplified femtosecond laser pulses. *J. Opt. Soc. Am. B* **1997**, *14*, 2348.
(51) Fetterman, M.; Goswami, D.; Keusters, D.; Yang, W.; Rhee, J.-K.; Warren, W. Ultrafast pulse shaping: amplification and characterization. *Opt. Express* **1998**, *3*, 366.

https://doi.org/10.1021/acs.jpclett.1c02481
J. Phys. Chem. Lett. 2021, 12, 8302−8308